Journal of Applied Analysis and Computation
Volume 11, Number 3, June 2021, 1557–1576
Website:http://www.jaac-online.com
DOI:10.11948/20200282

TWO-DIMENSIONAL ATTRACTING TORUS IN AN INTRAGUILD PREDATION MODEL WITH GENERAL FUNCTIONAL RESPONSES AND LOGISTIC GROWTH RATE FOR THE PREY

Gamaliel Blé[1,†] and Iván Loreto–Hernández[2]

Abstract The population coexistence in an intraguild food web model is analyzed. Three populations, the prey, the predator and super predator, are considered, where these last two populations are specialists. The sufficient conditions to guarantee a coexistence point, where the intraguild predation model exhibits a zero-Hopf bifurcation, are given. For a wide family of functional responses, these conditions are valid. The numerical simulations varying the functional responses are given. Different limit sets such as, limit cycles or invariant torus are shown.

Keywords Zero-Hopf bifurcation, attracting torus, intraguild predation model.

MSC(2010) 37G15, 37C75, 92D25, 92D40.

1. Introduction

One of the modules of intraguild predation (IGP) is the interaction in which a super predator simultaneously competes and predates with an intermediate predator, and they share the same resource [17]. This type of interaction is common in nature, and different mathematical models have been proposed in the literature to predict the extinction or coexistence of the involved populations. In fact, the works show conditions for which the generalist super predators may provide biocontrol service in an agroecosystem, see [11, 15, 16] and the references there in. On the other hand, assuming that the carrying capacity of the environment is dependent on the availability of a biotic resource, and both predators consume it, the Lotka-Volterra system has been modified to obtain the following system of differential equations to model IGP,

$$\frac{dx}{dt} = h_1(x) - f_1(x)y - f_2(x)z,$$

[†]The corresponding author.
Emails: gble@ujat.mx (G. Blé), iloretohe@conacyt.mx(I. Loreto–Hernández)
[1]División Académica de Ciencias Básicas, Universidad Juárez Autónoma de Tabasco, Km 1, Carretera Cunduacán–Jalpa de Méndez, Cunduacán, Tabasco, C.P. 86690, México
[2]División Académica de Ciencias Básicas, Consejo Nacional de Ciencia y Tecnología–Universidad Juárez Autónoma de Tabasco, Km 1, Carretera Cunduacán–Jalpa de Méndez, Cunduacán, Tabasco, C.P. 86690, México

$$\frac{dy}{dt} = r_1 y \left(1 - \frac{y}{px}\right) - f_3(y)z, \tag{1.1}$$
$$\frac{dz}{dt} = r_1 z \left(1 - \frac{z}{qx}\right) + c_3 f_3(y)z,$$

where x represents the density of a resourse (prey) that gets eaten by a predator of density y and a super predator z, and the species y feeds the super predator z. The function $h_1(x)$ represents the growth rate of the prey population in absence of the predators. The function $f_1(x)$ is the functional response of the predator to the prey. The functions $f_2(x)$ and $f_3(y)$ are the functional responses of the super predator to the prey and the predator, respectively.

Safuan *et al* studied the system (1.1) taking $h_1(x)$ as logistic map and the functional responses $f_1(x)$, $f_2(x)$ and $f_3(y)$ as Holling I (Lotka-Volterra). They showed stability, bifurcation and illustrated the system's dynamical behaviour using numerical simulations [18]. Capone *et al* generalized the Safuan's model taking $f_3(y)$ as Holling II. They studied the existence of absorbing sets in the phase space and the stability of a coexistence equilibrium point. Moreover, they showed numerical simulations on different regimes of coexistence and extinction of the involved populations [1].

On the other hand, if the benefit of the resource is not considered in the carrying capacity, we have the following system

$$\begin{aligned}
\frac{dx}{dt} &= \rho x(1 - x/k) - f_1(x)y - f_2(x)z, \\
\frac{dy}{dt} &= c_1 y f_1(x) - f_3(y)z - d_1 y, \\
\frac{dz}{dt} &= z(c_2 f_2(x) + c_3 f_3(y) - d_2),
\end{aligned} \tag{1.2}$$

where variables and functions are like in system (1.1). All parameters are positives; c_i and d_j are the conversion efficiency and the death rate, respectively, for $i = 1, 2, 3$ and $j = 1, 2$.

Holt and Polis studied the system (1.2) taking the functional responses $f_1(x)$,$f_2(x)$ and $f_3(y)$ as Holling I. They showed the stability of the equilibrium points, general criteria for the coexistence and the increased likelihood of unstable population dynamics with systems involving IGP [9].

Kang and Wedekin analyzed the system (1.2) taking the functional response $f_1(x)$ and $f_2(x)$ as Holling I, and $f_3(y)$ as Holling III. In addition, they studied a second model taking the same functional responses but considering a generalist super predator with a logistic growth function. They provided sufficient conditions, for the coexistence or extinction of a population, for these two models. Moreover, they determined the number of coexistence points of IGP models with generalist or specialist predator and studied their possible multiple attractors [10].

Castillo–Santos *et al* studied the differential system (1.2) with f_1, f_2 and f_3 as Holling II and they proved the existence of a stable limit cycle via a supercritical Andronov–Hopf bifurcation, which is valid under certain parameter conditions of the system [3].

Sen *et al* generalized the system (1.2) taking the functional response $f_1(x)$ and $f_2(x)$ as Holling I, and $f_3(y)$ as Holling II. They included the intraspecific competition for the predator and super predator populations. They investigated the local stability and bifurcation of all axial and boundary equilibrium points. Numerically, they showed the existence of a coexistence equilibrium point, a stable limit cycle bifurcating from this equilibrium point and chaos appearing via successive period doubling bifurcations [19].

Recently, Mendonça *et al* analyze the system (1.2) with $f_1(x)$ and $f_2(x)$ as Holling I, and $f_3(y)$ is a function considering refuge or defense mechanisms of the predator. Explicitly they study $f_3(y) = a_1 y^{n+1}$ or $f_3(y,z) = \frac{a_1 y}{1+a_2 z^m}$, and they provide conditions for coexistence of populations or extinction of one of them, and how nonlinearity influences [14].

A technique that has been used to determine the existence of limit cycles in a predator prey system is the zero-Hopf bifurcation. In [2] is applied to study a tritrophic food chain system, when the prey has a Malthusian growth rate and the functional responses are Holling type III; the limit cycles are found using the averaging theory of first order. More later, the averaging theory of second order is applied to determine limit cycles in a Volterra-Gause system [5]. In [22], the authors study an age-dependent predator prey system considering a Monod-Haldane functional response (Holling type IV) and a strong Allee effect. They proved that the system exhibits a zero-Hopf bifurcation near the coexistence steady state. In [20] is investigated the zero-Hopf bifurcation in a delayed predator prey model with dormancy of predators and it is used to explain the coexistence phenomena of several locally stable states, such as the coexistence of multiperiodic orbits, as well as the coexistence of a locally stable equilibrium and a locally stable periodic orbit.

In this work we analyze the system (1.2), and we show conditions that guarantee the coexistence of species for a wide family of functional responses. We give parameter conditions so that the system (1.2) exhibits a zero-Hopf bifurcation and consequently has different coexistence limit sets [6, 7, 12]. In particular, we give examples, taking $f_1(x)$ and $f_3(y)$ Holling I or III and $f_2(x)$ Holling II, III or IV, where this bifurcation appears. The numerical simulations show the existence of limit cycles and invariant torus in the phase space. In the works cited above, the zero-Hopf bifurcation is only used to determine limit cycles. Hence, the existence of invariant torus is the first time that the phenomena is shown in the literature related with food chain models in $\mathbb{R}^3$.

For ecological considerations we focus in finding stable solutions in the positive octant

$$\Omega = \{(x, y, z) \in \mathbb{R}^3 : x > 0, y > 0, z > 0\}.$$

2. Zero-Hopf bifurcation analysis

In this paper we assume $f_1, f_2, f_3 \in \mathcal{C}^3(\mathbb{R}^+)$, f_1, f_2, f_3 are positive functions in $\mathbb{R}^+$ and $f_1(0) = f_2(0) = f_3(0) = 0$. These last conditions guarantee the invariance of the positive octant Ω.

Proposition 2.1. *If $p = (x_0, y_0, z_0) \in \Omega$, and the parameters c_1, d_2 and ρ of the differential system* (1.2) *satisfy*

$$c_1 = \frac{d_1 y_0 + z_0 f_3(y_0)}{y_0 f_1(x_0)},\ d_2 = c_2 f_2(x_0) + c_3 f_3(y_0),\ \textit{and } \rho = \frac{y_0 f_1(x_0) + z_0 f_2(x_0)}{x_0(1 - x_0/k)}, \tag{2.1}$$

then p is an equilibrium point of the differential system (1.2) .

Proof. A point $p = (x_0, y_0, z_0) \in \Omega$ is an equilibrium point of the differential system (1.2) if and only if it satisfies the following system

$$\begin{aligned}
&\rho x_0(1 - x_0/k) - y_0 f_1(x_0) - z_0 f_2(x_0) = 0,\\
&- d_1 y_0 + c_1 y_0 f_1(x_0) - z_0 f_3(y_0) = 0,\\
&d_2 - c_2 f_2(x_0) - c_3 f_3(y_0) = 0.
\end{aligned}$$

Hence, a direct substitution of c_1, d_2 and ρ proves the result. □

In order to get positiveness on the parameters of the system, we assume from now on, and throughout this section, that $p = (x_0, y_0, z_0) \in \Omega$ and it satisfies

Condition A. $f_1'(x_0) > 0$, $f_2'(x_0) > 0$ and $f_3'(y_0) > 0$.

Moreover, we will assume that the parameters c_1, d_2 and ρ satisfy (2.1) in Proposition 2.1.

Next result provide us necessary conditions to have a zero-Hopf bifurcation for the differential system (1.2) at the equilibrium point p.

Lemma 2.1. *Let $p = (x_0, y_0, z_0) \in \Omega$, if*

$$f_1(x_0) - x_0 {f_1}'(x_0) = 0, \quad f_2(x_0) - x_0 {f_2}'(x_0) > 0, \quad f_3(y_0) - y_0 {f_3}'(y_0) = 0, \tag{2.2}$$

$$k = k_0 := \frac{x_0\left(x_0 y_0 {f_1}'(x_0) + x_0 z_0 {f_2}'(x_0) + 2k_2 z_0\right)}{k_2 z_0} \text{ and } c_3 = c_{30} := \frac{c_2 x_0^2 {f_1}'(x_0) {f_2}'(x_0)}{(x_0 {f_2}'(x_0) + k_2)(d_1 + z_0 {f_3}'(y_0))}, \tag{2.3}$$

then, the eigenvalues of the linear approximation of system (1.2) *at the equilibrium point $p = (x_0, y_0, z_0)$ are*

$$0 \text{ and } \pm i\omega_0, \tag{2.4}$$

where,

$$\omega_0 := \sqrt{\frac{y_0 {f_1}'(x_0)\eta + c_2 z_0 {f_2}'(x_0)\left(x_0 {f_2}'(x_0) + k_2\right)^2 \left(d_1 + z_0 {f_3}'(y_0)\right)}{\left(x_0 {f_2}'(x_0) + k_2\right)\left(d_1 + z_0 {f_3}'(y_0)\right)}}, \tag{2.5}$$

$$\eta = x_0 {f_2}'(x_0)\left(z_0 {f_3}'(y_0)\left((c_2 x_0 + z_0){f_3}'(y_0) + 2d_1\right) + d_1^2\right) + k_2\left(d_1 + z_0 {f_3}'(y_0)\right)^2$$

and $k_2 := f_2(x_0) - x_0 {f_2}'(x_0)$.

Proof. We notice that the characteristic polynomial $P(\lambda) = \lambda^3 + A_1\lambda^2 + A_2\lambda + A_3$ of the Jacobian matrix $M(p)$ of the differential system (1.2) evaluated at the equilibrium point p, has a zero root and a pair of purely imaginary roots $\pm i\omega_0$ if and only if $A_2 > 0$ and $A_1 = A_3 = 0$, where $\omega_0 = \sqrt{A_2}$.

Since conditions (2.2) hold, then

$$M(p) = \begin{pmatrix} M_{11} & -x_0 {f_1}'(x_0) & -x_0 {f_2}'(x_0) - k_2 \\ \frac{d_1 y_0 + y_0 z_0 {f_3}'(y_0)}{x_0} & 0 & -y_0 {f_3}'(y_0) \\ c_2 z_0 {f_2}'(x_0) & c_3 z_0 {f_3}'(y_0) & 0 \end{pmatrix},$$

where

$$M_{11} = -\frac{x_0 y_0 {f_1}'(x_0) + z_0\left(x_0 {f_2}'(x_0) + k_2\right)}{k\left(1 - \frac{x_0}{k}\right)} + \frac{x_0 y_0 {f_1}'(x_0) + z_0\left(x_0 {f_2}'(x_0) + k_2\right)}{x_0}$$

$$- y_0 {f_1}'(x_0) - z_0 {f_2}'(x_0).$$

And the coefficients of characteristic polynomial are

$$A_1 = \frac{k_2 z_0 (k - 2x_0) - x_0^2 \left(y_0 {f_1}'(x_0) + z_0 {f_2}'(x_0)\right)}{x_0(x_0 - k)},$$

$$A_2 = c_2 z_0 {f_2}'(x_0) \left(x_0 {f_2}'(x_0) + k_2\right) + c_3 y_0 z_0 {f_3}'(y_0)^2 + y_0 {f_1}'(x_0) \left(d_1 + z_0 {f_3}'(y_0)\right)$$

and

$$A_3 = \frac{y_0 z_0 {f_3}'(y_0)\Big((k - x_0)\big(x_0 {f_2}'(x_0)\big(c_2 x_0 {f_1}'(x_0) - c_3 d_1\big) - c_3 d_1 k_2\big) - c_3 x_0 {f_3}'(y_0)\big(x_0 y_0 {f_1}'(x_0) + z_0\big(k {f_2}'(x_0) + k_2\big)\big)\Big)}{x_0(x_0 - k)}.$$

Hence, if the parameters k and c_3 satisfy (2.3) then $A_1 = A_3 = 0$ and $A_2 > 0$, thus the eigenvalues of the linear approximation of system (1.2), at the equilibrium point p, are given by (2.4)–(2.5). □

Applying the Guckenheimer-Kuznetsov formula, (see [7,12]) and using the Mathematica software, we compute the terms $S(p, k_0, c_{30}) := B(p, k_0, c_{30})C(p, k_0, c_{30})$, $\Theta(p, k_0, c_{30})$ and $E(p, k_0, c_{30})$, which are necessary to guaranty the first nondegeneracy zero-Hopf bifurcation condition of the differential system (1.2) at the equilibrium point p. In summary we have.

Lemma 2.2. *If the hypotheses of Lemma 2.1 hold, then the terms $S(p, k_0, c_{30})$ and $\Theta(p, k_0, c_{30})$ of the differential system* (1.2) *at the equilibrium point p are*

$$S(p, k_0, c_{30}) = -\frac{y_0 f_2(x_0)\big(d_1 + z_0 f_3'(y_0)\big)\sigma_1\sigma_2}{2x_0^2 f_1'(x_0) f_2'(x_0)^2\big(f_2(x_0)^2\big(d_1 + z_0 f_3'(y_0)\big) + x_0^2 y_0 f_1'(x_0) f_3'(y_0)^2\big)\sigma_3^2},$$

$$\Theta(p, k_0, c_{30}) = \frac{f_1'(x_0)\big(d_1 + z_0 f_3'(y_0)\big)\big(f_2(x_0)^2\theta_1 - x_0 y_0 f_2(x_0)\theta_2 + \theta_3\big)}{c_2 z_0\Big(f_2(x_0)^2 f_2'(x_0) f_3''(y_0)\big(d_1 + z_0 f_3'(y_0)\big)^2\big(x_0 y_0 f_1'(x_0) + z_0 f_2(x_0)\big) + x_0^2 y_0 f_1'(x_0) f_3'(y_0)^2\theta_4\Big)},$$

where, $\sigma_1, \sigma_2, \sigma_3, \theta_1, \theta_2, \theta_3, \theta_4$ are given in the Appendix A.

$E(p, k_0, c_{30})$ is a very long term and we only put it in the examples below.

Now, we consider the vector field associated to the differential system (1.2),

$$\begin{aligned} F(\mathbf{x}, \alpha) =& (\rho x(1 - x/k) - f_1(x)y - f_2(x)z, c_1 y f_1(x) - f_3(y)z - d_1 y, \\ & z(c_2 f_2(x) + c_3 f_3(y) - d_2)), \end{aligned}$$

where $\mathbf{x} = (x, y, z)$ and $\alpha = (k, c_3)$.

Let Δ be the expression given in the Appendix B, we have the following result.

Lemma 2.3 (Second nondegeneracy condition, regularity)**.** *If conditions* (2.2) *are satisfied and $\Delta \neq 0$, then the map $\Psi(\mathbf{x}, \alpha) := (F(\mathbf{x}, \alpha), Tr\ F_{\mathbf{x}}(\mathbf{x}, \alpha), Det\ F_{\mathbf{x}}(\mathbf{x}, \alpha))$ is regular at (p, α_0), where $\alpha_0 = (k_0, c_{30})$.*

Proof. Under the hypotheses of Lemma 2.1, a direct computation using the Mathematica software shows that determinant of the derivative of the map Ψ at (p, α_0) is

$$\text{Det } D\Psi(p, \alpha_0) = \frac{c_2 k_2^2 y_0^2 z_0^4 f_3'(y_0)\Delta}{x_0^3\,(x_0 f_2'(x_0) + k_2)(d_1 + z_0 f_3'(y_0))(x_0 y_0 f_1'(x_0) + x_0 z_0 f_2'(x_0) + 2k_2 z_0)}.$$

Hence, the map Ψ is regular if $\Delta \neq 0$. □

Theorem 2.1. *If the equilibrium point $p = (x_0, y_0, z_0) \in \Omega$, is such that condition* (2.2) *is satisfied and $\Delta, S(p, k_0, c_{30}), \Theta(p, k_0, c_{30})$ and $E(p, k_0, c_{30})$ are nonzero then the differential system* (1.2) *exhibits a zero-Hopf bifurcation at p, with respect to the parameters (k, c_3) and its bifurcation value is $\alpha_0 = (k_0, c_{30})$.*

3. Examples

In this section, we show the existence of two-dimensional attracting torus for the differential system (1.2), for certain functional responses, which is important because implies the coexistence of the three species in a two-dimensional region.

We assume that the parameters $c_1,\ d_2$ and ρ satisfy (2.1) in Proposition 2.1. Moreover, we assume that the functional responses f_1, f_2 and f_3 are of Holling type I, II, III or IV, see [4, 8, 13, 21].

3.1. f_1 and f_3 Holling type III functional responses

In this subsection, we assume that the functional responses f_1 and f_3 are of Holling type III, explicitly we consider

$$f_i(s) = \frac{a_i s^2}{b_i + s^2}, \qquad \text{for } i = 1, 3.$$

Where $a_i > 0$ and $b_i > 0$, for $i = 1, 3$. Clearly $f_i(s) > 0$ and $f_i'(s) > 0$, for all $s > 0$, and $i = 1, 3$. Hence Condition **A** holds.

In this case $f_i(s) - s f_i'(s) = \frac{a_i\left(s^4 - b_i s^2\right)}{(b_i + s^2)^2}$, hence the first and third conditions in (2.2) are satisfied if

$$b_1 = x_0^2 \quad \text{and} \quad b_3 = y_0^2. \tag{3.1}$$

3.1.1. f_2 Holling type II

In this example we consider that the functional response f_2 is of Holling type II, explicitly we assume $f_2(x) = \frac{a_2 x}{b_2 + x}$, where a_2 and b_2 are positive. Clearly $f_2'(x) > 0$, for all $x > 0$, hence Condition **A** holds.

For this functional response we have $f_2(x) - x f_2'(x) = \frac{a_2 x^2}{(b_2 + x)^2}$, then second condition in (2.2) is satisfied.

Therefore, by Theorem 2.1 the differential system (1.2) exhibits a zero-Hopf bifurcation at p, with respect to the parameters (k, c_3) and its bifurcation value is (k_0, c_{30}), as long as the coefficients $\Delta, S(p, k_0, c_{30}), \Theta(p, k_0, c_{30})$ and $E(p, k_0, c_{30})$ are non zero. In order to simplify these last expressions, we assign the parameters z_0, a_2, b_2, c_2 and d_1 the values given in first column of Table 1.

Table 1. Parameter assignments.

Additional conditions	Conditions (2.1) in Proposition 2.1	Conditions (3.1)
$z_0 = \frac{a_1 y_0^2}{a_3 x_0}$, $a_2 = \frac{191 a_3 x_0}{500 y_0}$, $b_2 = \frac{x_0}{2}$, $c_2 = \frac{1687500 a_1 y_0^2}{213587 a_3 x_0^2}$, $d_1 = \frac{a_1 y_0}{2 x_0}$	$c_1 = \frac{2 y_0}{x_0}$, $d_2 = \frac{570375 a_1 y_0}{213587 x_0}$, $\rho = \frac{208 a_1 y_0}{225 x_0}$,	$b_1 = x_0^2$, $b_3 = y_0^2$

Moreover, the parameters c_1, d_2, ρ, b_1 and b_3 given by (2.1) and (3.1), take the values shown in the last columns of Table 1.

The equilibrium point is $p = \left(x_0, y_0, \frac{a_1 y_0^2}{a_3 x_0}\right)$, and the bifurcation value is $(k_0, c_{30}) = \left(\frac{1040 x_0}{191}, \frac{281250 a_1 y_0}{213587 a_3 x_0}\right)$, the eigenvalues of the linearization of the differential system at p are

$$0 \quad \text{and} \quad \pm i \frac{a_1 y_0}{x_0}.$$

The coefficients S, Θ, E and Δ take the values

$$S(p, k_0, c_{30}) = \frac{6690621377557a_3^2}{821149318242000000y_0^2}, \quad \Theta(p, k_0, c_{30}) = -\frac{299582705}{133731},$$

$$E(p, k_0, c_{30}) = \frac{4927860429898701627925604373 1a_1 y_0}{434067786006111088796250000 0x_0^3},$$

$$\text{and} \quad \Delta = \frac{67008233759a_1^3 a_3^4}{68343750000000y_0^2}.$$

We notice that S is positive and Θ negative, in this case a branch of torus bifurcation appears, which is transversal to the saddle-node and Andronov–Hopf bifurcation curves. The torus bifurcation generates an invariant two-dimensional torus, which disappears via a heteroclinic destruction, see [7, 12].

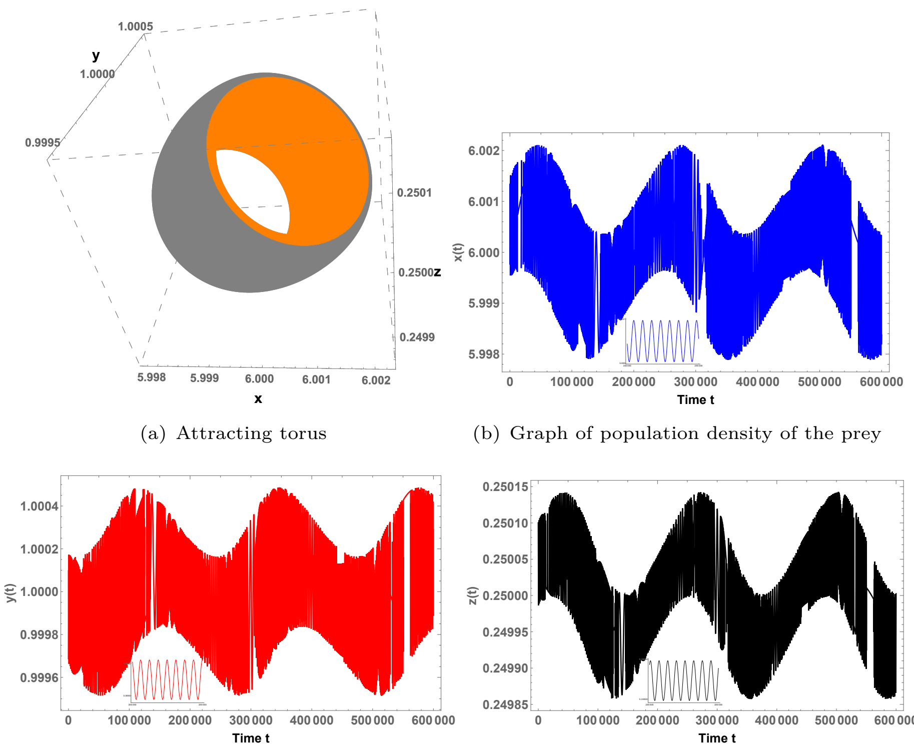

(a) Attracting torus

(b) Graph of population density of the prey

(c) Graph of population density of the predator

(d) Graph of population density of the super-predator

Figure 1. Attracting torus and graphs of population densities, taking $x_0 = 6$, $y_0 = 1$, $a_1 = 6$, $a_3 = 4$, $c_3 = c_{30} + \frac{1}{10^9}$ and $k = k_0 + \frac{4}{10^6}$.

We do the numerical simulations taking parameters values that exemplify the existence of an invariant torus, see Figure 1. The positive orbit with initial condition $q = (6.0001, 1.0001, 0.2501)$, in the phase space of the differential system (1.2) is shown in Figure 1 (a). As it can be seen, such orbit tends to an attracting two-dimensional torus as the time goes to infinity, this orbit starts at the bottom of the inner cylinder (orange orbit), going up swinging along the cylinder until it reaches the top, then it descends on the outside of the torus (gray orbit). In Figure 1 is shown the graphs of density population functions $x(t), y(t)$ and $z(t)$, in the interval of time $[0, 600000]$, which define the parametrized version of the above mentioned orbit. Each graph exhibits a time-periodic behavior, with small and big oscillations. A zoom is presented to show the small oscillations of the functions $x(t), y(t)$ and $z(t)$ in the interval of time $[200000, 200050]$, see Figure 1 (a), (b) and (c), respectively.

3.1.2. f_2 Holling type III

In this example we consider that the functional response f_2 is of Holling type III, explicitly we assume $f_2(x) = \frac{a_2 x^2}{b_2 + x^2}$, where a_2 and b_2 are positive. Clearly $f_2'(x) > 0$, for all $x > 0$, hence Condition **A** holds.

We have that $f_2(x_0) - x_0 f_2'(x_0) = \frac{a_2\left(x_0^4 - b_2 x_0^2\right)}{\left(b_2 + x_0^2\right)^2}$, then second condition in (2.2) is satisfied if $x_0^4 - b_2 x_0^2 > 0$.

Therefore, by Theorem 2.1 the differential system (1.2) exhibits a zero–Hopf bifurcation at p, with respect to the parameters (k, c_3) and its bifurcation value is (k_0, c_{30}), as long as the coefficients $\Delta, S(p, k_0, c_{30}), \Theta(p, k_0, c_{30})$ and $E(p, k_0, c_{30})$ are non zero. In order to simplify these last expressions, we assign the parameters z_0, a_2, b_2, c_2 and d_1 the values given in first column of Table 2.

Table 2. Parameter assignments.

Additional conditions	Conditions (2.1) in Proposition 2.1	Conditions (3.1)
$z_0 = \frac{a_1 y_0^2}{a_3 x_0}$, $a_2 = \frac{a_3 x_0}{4 y_0}$, $b_2 = \frac{x_0^2}{2}$, $c_2 = \frac{54 a_1 y_0^2}{11 a_3 x_0^2}$, $d_1 = \frac{a_1 y_0}{2 x_0}$	$c_1 = \frac{2 y_0}{x_0}$, $d_2 = \frac{18 a_1 y_0}{11 x_0}$, $\rho = \frac{13 a_1 y_0}{18 x_0}$	$b_1 = x_0^2$, $b_3 = y_0^2$

Moreover, the parameters c_1, d_2, ρ, b_1 and b_3 given by (2.1) and (3.1), take the values shown in the last columns of Table 2.

The equilibrium point is $p = \left(x_0, y_0, \frac{a_1 y_0^2}{a_3 x_0}\right)$, and the bifurcation value is $(k_0, c_{30}) = \left(13 x_0, \frac{18 a_1 y_0}{11 a_3 x_0}\right)$, the eigenvalues of the linearization of the differential system at p are

$$0 \quad \text{and} \quad \pm i \frac{a_1 y_0}{x_0}.$$

The coefficients S, Θ, E and Δ take the values

$$\begin{aligned} S(p, k_0, c_{30}) &= -\frac{6505 a_3^2}{418176 y_0^2}, \quad \Theta(p, k_0, c_{30}) = \frac{283}{135}, \\ E(p, k_0, c_{30}) &= -\frac{84518761 a_1 y_0}{111282336 x_0^3} \quad \text{and} \quad \Delta = \frac{167 a_1^3 a_3^4}{139968 y_0^2}. \end{aligned}$$

We notice that S is negative and Θ positive, in this case a branch of torus bifurcation appears, which is transversal to the saddle-node and Andronov–Hopf bifurcation curves. The torus bifurcation generates an invariant two-dimensional torus, which disappears via a blow-up, see [7, 12].

We do the numerical simulations taking parameters values that exemplify the existence of an invariant torus, see Figure 2. The positive orbit with initial condition $q = (3.0001, 1.0001, 0.2501)$, in the phase space of the differential system (1.2) is shown in Figure 2 (a). As it can be seen, such orbit tends to an attracting two-dimensional torus as the time goes to infinity. In Figure 3 we show the graphs of the functions $x(t), y(t)$ and $z(t)$, in the interval of time $[0, 100000]$, which define the

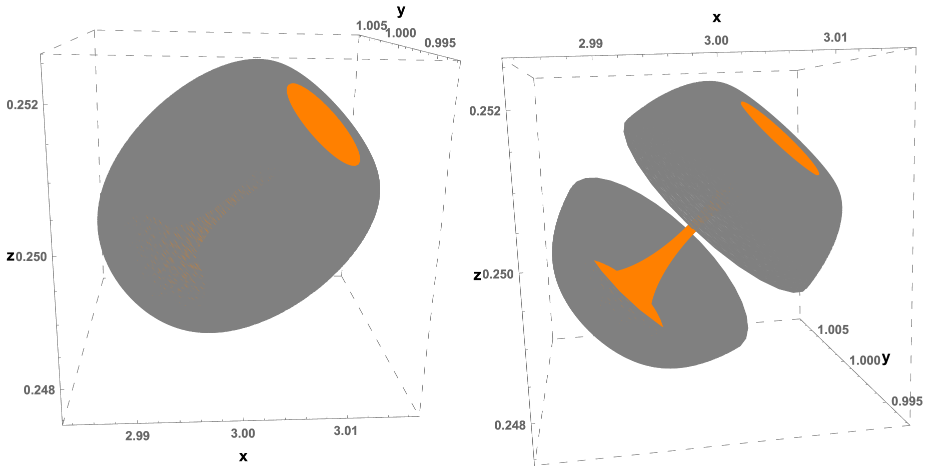

(a) Attracting torus (b) Internal part of attracting torus

Figure 2. Attracting torus, taking $x_0 = 3$, $y_0 = 1$, $a_1 = 3$, $a_3 = 4$, $c_3 = c_{30} + \frac{1}{10^6}$ and $k = k_0 - \frac{7}{10^4}$.

parametrized version of the above mentioned orbit. Each graph exhibits a time-periodic behavior, with small and big oscillations. A zoom is presented to show the small oscillations of the functions $x(t)$, $y(t)$ and $z(t)$ in the interval of time $[40000, 40050]$, see Figure 3.

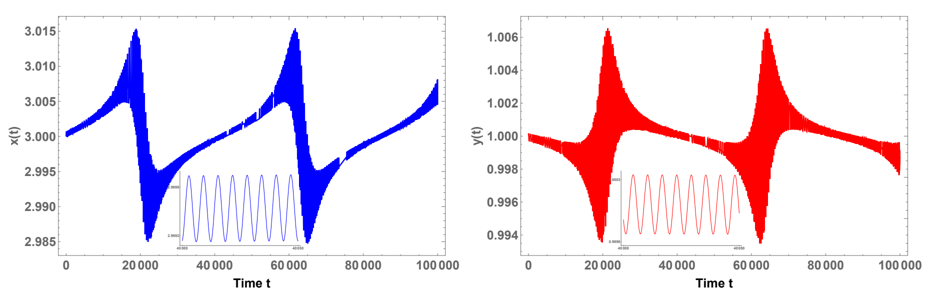

(a) Graph of population density of the prey (b) Graph of population density of the predator

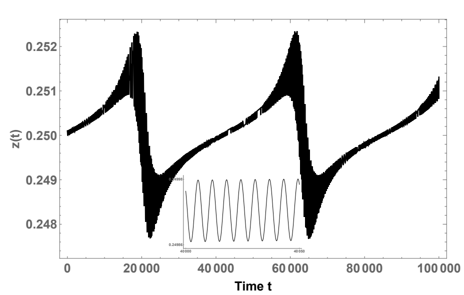

(c) Graph of population density of the super-predator

Figure 3. Time series of population densities

3.1.3. f_2 Holling type IV

In this example we consider that the functional response f_2 is of Holling type IV, explicitly we assume $f_2(x) = \frac{a_2 x}{b_2+x^2}$, where a_2 and b_2 are positive. Since $f_2'(x) = \frac{a_2\left(b_2-x_0^2\right)}{\left(b_2+x_0^2\right)^2}$, then, Condition **A** holds if $b_2 > x_0^2$.

We have that $f_2(x_0) - x_0 f_2'(x_0) = \frac{2a_2 x_0^3}{\left(b_2+x_0^2\right)^2}$, hence, second condition in (2.2) is satisfied.

Therefore, by Theorem 2.1 the differential system (1.2) exhibits a zero-Hopf bifurcation at p, with respect to the parameters (k, c_3) and its bifurcation value is (k_0, c_{30}), as long as the coefficients $\Delta, S(p, k_0, c_{30}), \Theta(p, k_0, c_{30})$ and $E(p, k_0, c_{30})$ are non zero. In order to simplify these last expressions, we assign the parameters z_0, a_2, b_2, c_2 and d_1 the values given in first column of Table 3. Moreover, the parameters c_1, d_2, ρ, b_1 and b_3 given by (2.1) and (3.1), take the values shown in the last columns of Table 3.

Table 3. Parameter assignments.

Additional conditions	Conditions (2.1) in Proposition 2.1	Conditions (3.1)
$z_0 = \frac{a_1 y_0^2}{a_3 x_0}$, $a_2 = \frac{4a_3 x_0^2}{25 y_0}$, $b_2 = \frac{3x_0^2}{2}$, $c_2 = \frac{312500 a_1 y_0^2}{16137 a_3 x_0^2}$, $d_1 = \frac{a_1 y_0}{2x_0}$	$c_1 = \frac{2y_0}{x_0}$, $d_2 = \frac{11875 a_1 y_0}{5379 x_0}$, $\rho = \frac{769 a_1 y_0}{1250 x_0}$	$b_1 = x_0^2$, $b_3 = y_0^2$

The equilibrium point is $p = \left(x_0, y_0, \frac{a_1 y_0^2}{a_3 x_0}\right)$, and the bifurcation value is $(k_0, c_{30}) = \left(\frac{769 x_0}{64}, \frac{31250 a_1 y_0}{16137 a_3 x_0}\right)$, the eigenvalues of the linearization of the differential system at p are

$$0 \quad \text{and} \quad \pm i \frac{a_1 y_0}{x_0}.$$

The coefficients S, Θ, E and Δ take the values

$$S(p, k_0, c_{30}) = -\frac{483854357111123 a_3^2}{13020138450000000 y_0^2}, \quad \Theta(p, k_0, c_{30}) = \frac{1436903}{79975},$$
$$E(p, k_0, c_{30}) = \frac{25274984745814862991038 01 a_1 y_0}{114876967995290703125000000 x_0^3} \quad \text{and} \quad \Delta = \frac{57494851 a_1^3 a_3^4}{244140625000 y_0^2}.$$

We notice that S is negative and Θ positive, as in Example 3.1.2, a branch of torus bifurcation appears, which is transversal to the saddle-node and Andronov–Hopf bifurcation curves. The torus bifurcation generates an invariant two-dimensional torus, which disappears via a blow-up.

We do the numerical simulations taking parameters values that exemplify the existence of an invariant torus, see Figure 4. The positive orbit with initial condition $q = (10.0001, 1.0001, 0.2501)$, in the phase space of the differential system (1.2) is shown in Figure 4 (a). As it can be seen, such orbit tends to an attracting two-dimensional torus as the time goes to infinity. Also in Figure 4, we show the graph of the functions $x(t), y(t)$ and $z(t)$, in the time interval $[0, 50000]$, which define the parametrized version of the above mentioned orbit. Each graph exhibits a time-periodic behavior, with small and big oscillations. A zoom is presented to show the small oscillations of the functions $x(t), y(t)$ and $z(t)$ in the interval of time $[20000, 20050]$, see Figure 4 (b), (c) and (d), respectively.

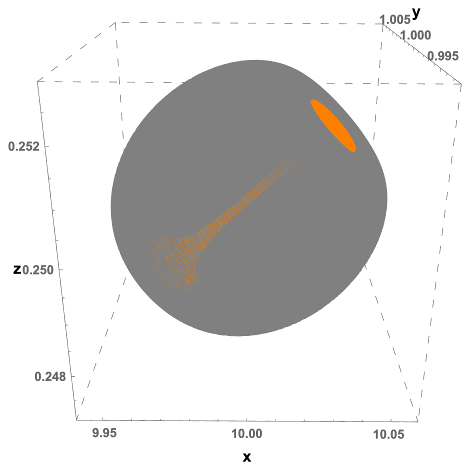

(a) Attracting torus

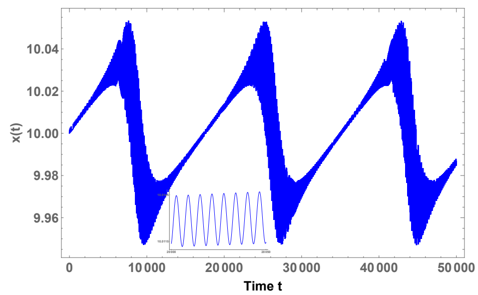

(b) Graph of population density of the prey

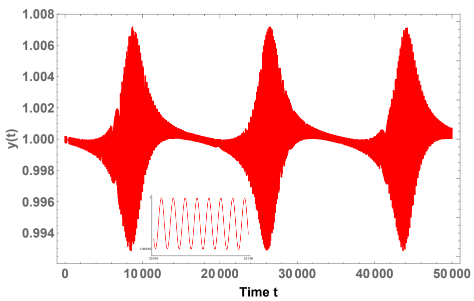

(c) Graph of population density of the predator

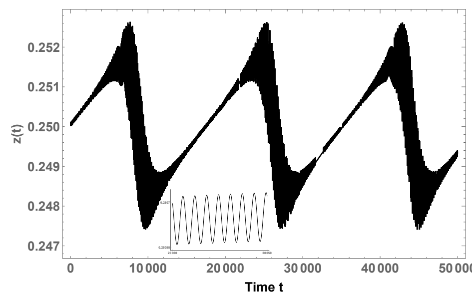

(d) Graph of population density of the super-predator

Figure 4. Attracting torus and graphs of population densities, taking $x_0 = 10$, $y_0 = 1$, $a_1 = 10$, $a_3 = 4$, $c_3 = c_{30} + \frac{1}{10^6}$ and $k = k_0 - \frac{1}{10^8}$.

Now, considering the small perturbation

$$k = k_0 - \frac{1}{10^6} \quad \text{and} \quad c_3 = c_{30} + \frac{1}{10^2},$$

the positive orbit with initial condition q, tends to a stable limit cycle, which is shown in Figure 5 (a). Also, we show the graph of the functions $x(t), y(t)$ and $z(t)$, in the interval of time $[0, 100000]$, each graph exhibits a time-periodic behavior. A zoom is presented to appreciate the oscillations of the functions $x(t), y(t)$ and $z(t)$ in the interval of time $[99900, 100000]$, see Figure 5 (b), (c) and (d), respectively.

3.2. f_1 and f_3 Holling type I functional responses

In this subsection, we assume that the functional responses f_1 and f_3 are of Holling type I, explicitly we consider

$$f_i(s) = a_i s, \qquad \text{for } i = 1, 3.$$

Where $a_i > 0$ for $i = 1, 3$. Clearly $f_i(s) > 0$ and $f_i'(s) > 0$, for all $s > 0$, and $i = 1, 3$. Hence Condition **A** holds.

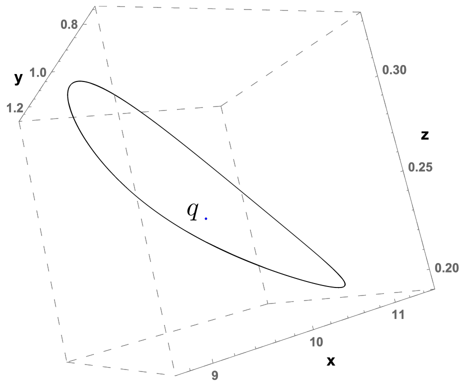

(a) Stable limit cycle

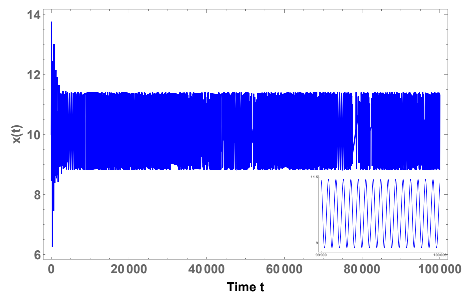

(b) Graph of population density of the prey

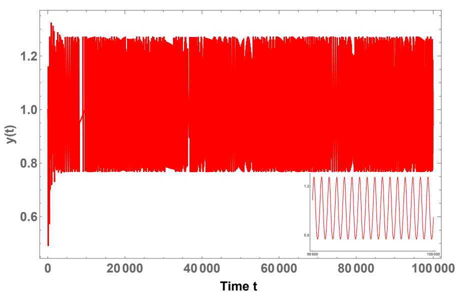

(c) Graph of population density of the predator

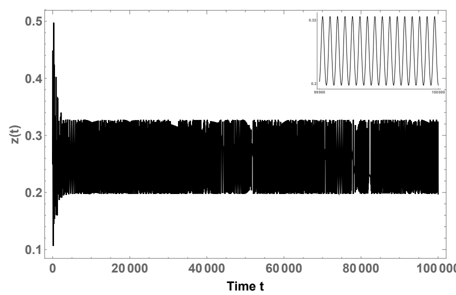

(d) Graph of population density of the super-predator

Figure 5. Stable limit cycle and time series

In this case $f_i(s) - sf_i'(s) = 0$, for all $s > 0$, and $i = 1, 3$. Hence the first and third conditions in (2.2) are satisfied.

3.2.1. f_2 Holling type II

In this example we consider that the functional response f_2 is as in Example 3.1.1, that is, $f_2(x) = \frac{a_2 x}{b_2 + x}$, where a_2 and b_2 are positive. Hence Condition **A** and second condition in (2.2) are satisfied.

Therefore, by Theorem 2.1 the differential system (1.2) exhibits a zero-Hopf bifurcation at p, with respect to the parameters (k, c_3) and its bifurcation value is (k_0, c_{30}), as long as the coefficients $\Delta, S(p, k_0, c_{30}), \Theta(p, k_0, c_{30})$ and $E(p, k_0, c_{30})$ are non zero. In order to simplify these last expressions, we assign the parameters z_0, a_2, b_2, c_2 and d_1 the values given in first column of Table 4. Moreover, the parameters c_1, d_2 and ρ given by (2.1), take the values shown in second column of Table 4.

Table 4. Parameter assignments.

Additional conditions	Conditions (2.1) in Proposition 2.1
$z_0 = \frac{a_1 y_0}{a_3}, \quad a_2 = 3a_3 x_0, \quad b_2 = x_0, \quad c_2 = \frac{16 a_1 y_0}{11 a_3 x_0}, \quad d_1 = a_1 y_0$	$c_1 = \frac{2y_0}{x_0}, \quad d_2 = \frac{28 a_1 y_0}{11}, \quad \rho = \frac{13 a_1 y_0}{4}$

The equilibrium point is $p = \left(x_0, y_0, \frac{a_1 y_0}{a_3}\right)$, and the bifurcation value is $(k_0, c_{30}) =$

$\left(\frac{13x_0}{3}, \frac{4a_1}{11a_3}\right)$, the eigenvalues of the linearization of the differential system at p are

$$0 \quad \text{and} \quad \pm\, 2ia_1y_0.$$

The coefficients S, Θ, E and Δ take the values

$$S(p,k_0,c_{30}) = \frac{243a_3^2}{7744}, \quad \Theta(p,k_0,c_{30}) = -12,$$
$$E(p,k_0,c_{30}) = \frac{5831a_1y_0}{25344x_0^2} \quad \text{and} \quad \Delta = \frac{45}{16}a_1^3a_3^4x_0^3y_0^2.$$

We notice that S is positive and Θ negative, as in Example 3.1.1, hence, a branch of torus bifurcation appears, which is transversal to the saddle-node and Andronov–Hopf bifurcation curves. The torus bifurcation generates an invariant two-dimensional torus, which disappears via a heteroclinic destruction.

We do the numerical simulations taking parameters values that exemplify the existence of an invariant torus, see Figure 6. The positive orbit with initial condition $q = (1.0001, 0.2501, 0.2501)$, in the phase space of the differential system (1.2) is shown in Figure 6 (a).

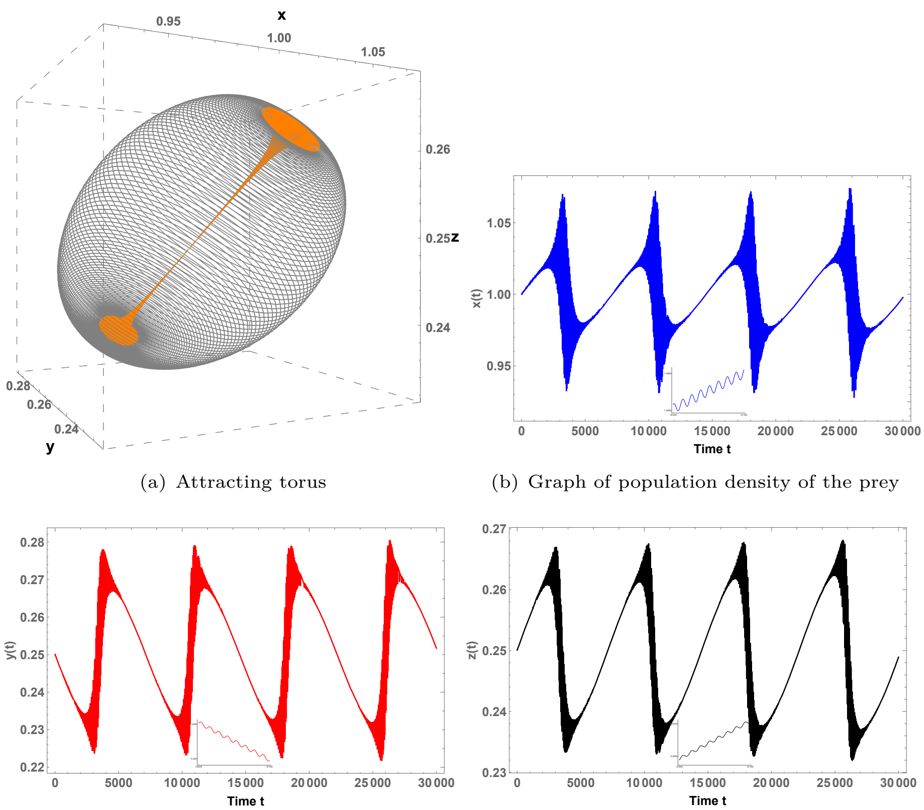

(a) Attracting torus

(b) Graph of population density of the prey

(c) Graph of population density of the predator

(d) Graph of population density of the super-predator

Figure 6. Attracting torus and graphs of population densities, taking $x_0 = 1$, $y_0 = \frac{1}{4}$, $a_1 = 1$, $a_3 = 1$, $c_3 = c_{30} - \frac{1}{10^6}$ and $k = k_0 + \frac{3}{10^3}$.

As it can be seen, such orbit tends to an attracting two-dimensional torus as the time goes to infinity. Also in Figure 6 is shown the graph of the functions $x(t), y(t)$ and $z(t)$, in the time interval $[0, 30000]$, which define the parametrized version of the above mentioned orbit. Each graph exhibits a time–periodic behavior, with small and big oscillations. A zoom is presented to show the small oscillations of the functions $x(t), y(t)$ and $z(t)$ in the interval of time $[15000, 15100]$, see Figure 6 (b), (c) and (d), respectively.

3.2.2. f_2 Holling type III

In this example we consider that the functional response f_2 is as in Example 3.1.2, that is, $f_2(x) = \frac{a_2x^2}{b_2+x^2}$, where a_2 and b_2 are positive. Hence Condition **A** holds and taking $b_2 = \frac{x_0^2}{2}$ second condition in (2.2) is satisfied.

Therefore, by Theorem 2.1 the differential system (1.2) exhibits a zero-Hopf bifurcation at p, with respect to the parameters (k, c_3) and its bifurcation value is (k_0, c_{30}), as long as the coefficients $\Delta, S(p, k_0, c_{30}), \Theta(p, k_0, c_{30})$ and $E(p, k_0, c_{30})$ are non zero. In order to simplify these last expressions, we assign the parameters z_0, a_2, b_2, c_2 and d_1 the values given in first column of Table 5. Moreover, the parameters c_1, d_2 and ρ given by (2.1), take the values shown in second column of Table 5.

Table 5. Parameter assignments.

Additional conditions	Conditions (2.1) in Proposition 2.1
$z_0 = \frac{a_1y_0}{a_3}$, $a_2 = a_3x_0$, $c_2 = \frac{54a_1y_0}{17a_3x_0}$, $d_1 = a_1y_0$	$c_1 = \frac{2y_0}{x_0}$, $d_2 = \frac{54a_1y_0}{17}$, $\rho = \frac{17a_1y_0}{9}$

The equilibrium point is $p = \left(x_0, y_0, \frac{a_1y_0}{a_3}\right)$, and the bifurcation value is $(k_0, c_{30}) = \left(\frac{17x_0}{2}, \frac{18a_1}{17a_3}\right)$, the eigenvalues of the linearization of the differential system at p are

$$0 \quad \text{and} \quad \pm 2ia_1y_0.$$

The coefficients S, Θ, E and Δ become

$$\begin{aligned} S(p, k_0, c_{30}) &= \frac{2653a_3^2}{46818}, \quad \Theta(p, k_0, c_{30}) = -\frac{233}{63}, \\ E(p, k_0, c_{30}) &= \frac{69609059a_1y_0}{87676344x_0^2} \quad \text{and} \quad \Delta = \frac{896}{729}a_1^3a_3^4x_0^3y_0^2. \end{aligned}$$

We notice that S is positive and Θ negative, as in Examples 3.1.1 and 3.2.1, hence, a branch of torus bifurcation appears. This torus bifurcation generates an invariant two-dimensional torus, which disappears via a heteroclinic destruction.

We do the numerical simulations taking parameters values that exemplify the existence of an invariant torus, see Figure 7. The positive orbit with initial condition $q = (1.0001, 0.2501, 0.0501)$, in the phase space of the differential system (1.2) is shown in Figure 7 (a).

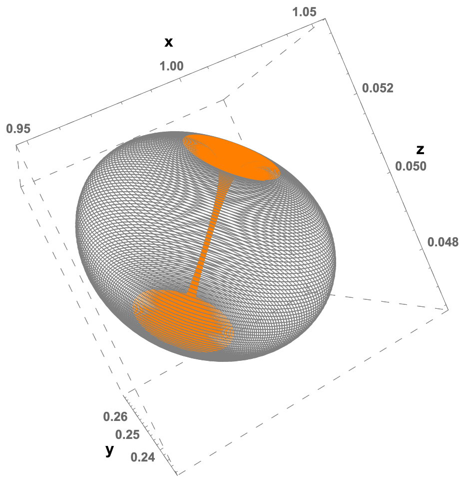

(a) Attracting torus

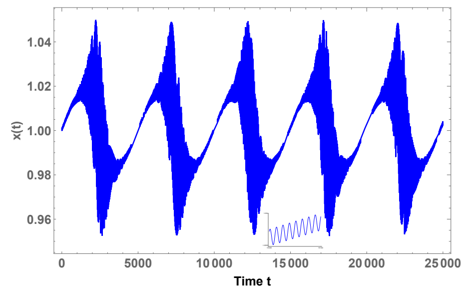

(b) Graph of population density of the prey

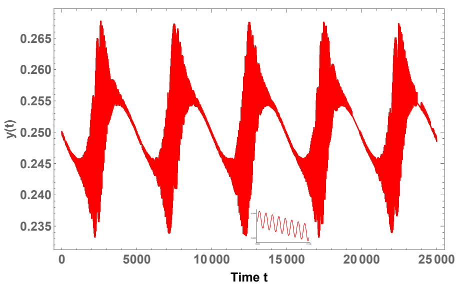

(c) Graph of population density of the predator

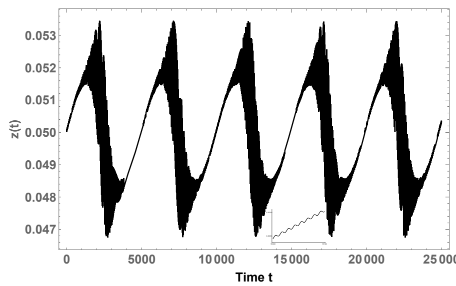

(d) Graph of population density of the super-predator

Figure 7. Attracting torus and graphs of population densities, taking $x_0 = 1$, $y_0 = \frac{1}{4}$, $a_1 = 1$, $a_3 = 5$, $c_3 = c_{30} + \frac{1}{10^6}$ and $k = k_0 + \frac{1}{10^2}$.

As it can be seen, such orbit tends to an attracting two-dimensional torus as the time goes to infinity. Also in Figure 7 is shown the graph of density population functions $x(t), y(t)$ and $z(t)$, in the time interval $[0, 25000]$, which define the parametrized version of the above mentioned orbit. Each graph exhibits a time–periodic behavior, with small and big oscillations. A zoom is presented to show the small oscillations of the functions $x(t), y(t)$ and $z(t)$ in the interval of time $[15000, 15100]$, see Figure 7 (b), (c) and (d), respectively.

3.2.3. f_2 Holling type IV

In this example we consider that the functional response f_2 is as in Example 3.1.3, that is, $f_2(x) = \frac{a_2 x}{b_2 + x^2}$, where a_2 and b_2 are positive. Hence second condition in (2.2) is satisfied. Setting $b_2 = 2x_0^2$ condition **A** holds.

Therefore, by Theorem 2.1 the differential system (1.2) exhibits a zero-Hopf bifurcation at p, with respect to the parameters (k, c_3) and its bifurcation value is (k_0, c_{30}), as long as the coefficients $\Delta, S(p, k_0, c_{30}), \Theta(p, k_0, c_{30})$ and $E(p, k_0, c_{30})$ are non zero. In order to simplify these last expressions, we assign the parameters z_0, a_2, b_2, c_2 and d_1 the values given in first column of Table 6. Moreover, the parameters c_1, d_2 and ρ given by (2.1), take the values shown in second column of Table 6.

Table 6. Parameter assignments.

Additional conditions	Conditions (2.1) in Proposition 2.1
$z_0 = \frac{a_1 y_0}{a_3}$, $a_2 = a_3 x_0^2$, $c_2 = \frac{108 a_1 y_0}{11 a_3 x_0}$, $d_1 = a_1 y_0$.	$d_2 = \frac{54 a_1 y_0}{11}$, $\rho = \frac{14 a_1 y_0}{9}$, $c_1 = \frac{2 y_0}{x_0}$.

The equilibrium point is $p = \left(x_0, y_0, \frac{a_1 y_0}{a_3}\right)$, and the bifurcation value is $(k_0, c_{30}) = \left(7x_0, \frac{18 a_1}{11 a_3}\right)$, the eigenvalues of the linearization of the differential system at p are

$$0 \quad \text{and} \quad \pm 2ia_1 y_0.$$

The coefficients S, Θ, E and Δ become

$$\begin{aligned} S(p, k_0, c_{30}) &= \frac{9709 a_3^2}{78408}, \quad \Theta(p, k_0, c_{30}) = -\frac{281}{171}, \\ E(p, k_0, c_{30}) &= \frac{981731 a_1 y_0}{415234512 x_0^2} \quad \text{and} \quad \Delta = \frac{164}{729} a_1^3 a_3^4 x_0^3 y_0^2. \end{aligned}$$

We notice that S is positive and Θ negative, hence, a branch of torus bifurcation appears. This torus bifurcation generates an invariant two-dimensional torus, which disappears via a heteroclinic destruction.

We do the numerical simulations taking parameters values that exemplify the existence of an invariant torus, see Figure 8. The positive orbit with initial condition $q = (1.0001, 0.2501, 0.0501)$, in the phase space of the differential system (1.2) is shown in Figure 8 (a). As it can be seen, such orbit tends to an attracting two-dimensional torus as the time goes to infinity. Also in Figure 8 (b), (c) and (d) are shown the graphs of density population functions $x(t), y(t)$ and $z(t)$, respectively, which define the parametrized version of the above mentioned orbit. Each graph exhibits a time-periodic behavior, with small and big oscillations.

4. Conclusions

The results obtained show parameter conditions for which the intraguild system (1.2) has a coexistence equilibrium point and it exhibits a zero-Hopf bifurcation. The bifurcation parameters are the carrying capacity k for the prey and conversion efficiency c_3 of the super predator when it consumes the predator. The presence of a zero-Hopf bifurcation in the system (1.2) shows the complexity that the coexistence of three species can present, which not only stabilizes around an equilibrium point or a limit cycle, but can also be around an invariant torus or an invariant sphere. Thus, the population values oscillate around the values of each of these limit sets, depending of parameter values in the system. Numerical simulations show these different limit sets and how the invariant torus tends to the invariant sphere. In particular, this simulation shows that coexistence in an intraguild predation model can be stabilized in more complicated limit sets than an equilibrium point or a periodic orbit. In the numerical simulations we have fixed the functional responses that measure the consumption of the predator to the prey and from the

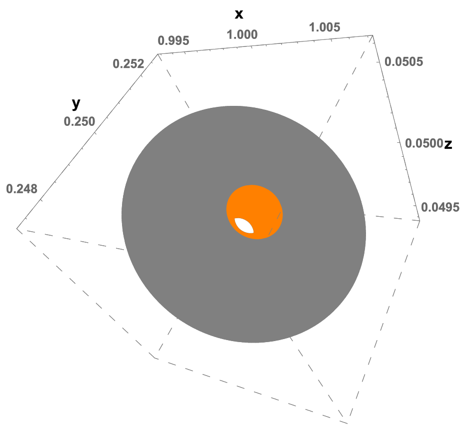

(a) Attracting torus

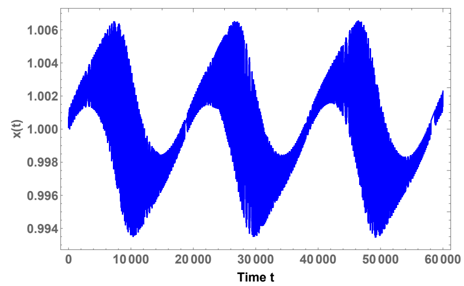

(b) Graph of population density of the prey

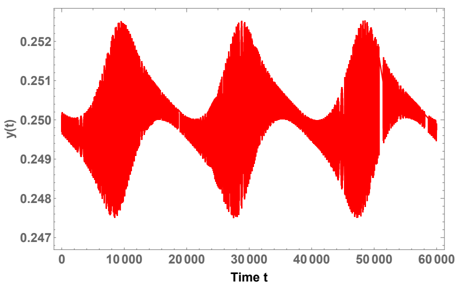

(c) Graph of population density of the predator

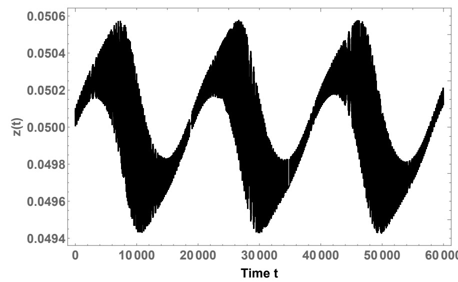

(d) Graph of population density of the superpredator

Figure 8. Attracting torus and graphs of population densities, taking $x_0 = 1$, $y_0 = \frac{1}{4}$, $a_1 = 1$, $a_3 = 5$, $c_3 = c_{30} - \frac{1}{10^7}$ and $k = k_0 + \frac{3}{10^4}$.

superpredator to the predator. We can observe that when they are Holling III (the predator spends a certain amount of time to ingest and capture their preys and has some form of learning behavior), coexistence occurs in better conditions for the superpredator than when they are Holling I (the predator consume their prey at a rate proportional to their rate of encounter). This occurs regardless of the Holling type that is taken as the functional response of the super predator to the primary resource.

Acknowledgment

We thank the referees for their valuable comments, which allowed us to improve this work.

Disclosure statement

No potential conflict of interest was reported by the authors.

A. First nondegeneracy condition

$$
\begin{aligned}
\sigma_1 =& - x_0 y_0 f_2(x_0)^2 f_1'(x_0) f_2'(x_0) f_3''(y_0) \left(d_1 + z_0 f_3'(y_0)\right)^2 \\
&+ x_0^3 y_0 f_1'(x_0)^2 f_2'(x_0) f_3'(y_0)^2 \left(2 d_1 f_2'(x_0) + x_0 f_3'(y_0) \left(y_0 f_1''(x_0) + z_0 f_2''(x_0)\right)\right) \\
&+ x_0^2 y_0 f_2(x_0) f_1'(x_0) f_3'(y_0)^2 (x_0 f_1''(x_0) f_2'(x_0) \left(d_1 + z_0 f_3'(y_0)\right) - f_1'(x_0)(x_0 f_2''(x_0) \\
&\times \left(d_1 + z_0 f_3'(y_0)\right) + 2 d_1 f_2'(x_0))) \\
&- z_0 f_2(x_0)^3 f_2'(x_0) f_3''(y_0) \left(d_1 + z_0 f_3'(y_0)\right)^2 , \\
\sigma_2 =& c_2 z_0 f_2(x_0)^3 f_2'(x_0) (x_0 f_1'(x_0) f_2''(x_0) \left(d_1 + z_0 f_3'(y_0)\right) \\
&- f_2'(x_0) (x_0 f_1''(x_0) \left(d_1 + z_0 f_3'(y_0)\right) + 2 z_0 f_1'(x_0) f_3'(y_0))) \\
&+ f_2(x_0)^2 f_1'(x_0) (f_2'(x_0) \sigma_{21} + y_0 f_1'(x_0) \left(d_1 + z_0 f_3'(y_0)\right) \\
&\times \left(x_0 f_2''(x_0) \left(d_1 + z_0 f_3'(y_0)\right) - 2 z_0 f_2'(x_0) f_3'(y_0)\right)) \\
&+ x_0 y_0 f_2(x_0) f_1'(x_0) f_2'(x_0) \left(f_1'(x_0) \sigma_{22} + c_2 x_0 z_0^2 f_2'(x_0) f_3'(y_0)^2 f_3''(y_0)\right) \\
&+ c_2 x_0^3 y_0 z_0 f_1'(x_0)^2 f_2'(x_0)^2 f_3'(y_0)^2 \left(2 f_2'(x_0) + y_0 f_3''(y_0)\right) , \\
\sigma_{21} =& - c_2 x_0^2 z_0 f_2'(x_0) f_3'(y_0) \left(y_0 f_1''(x_0) + z_0 f_2''(x_0)\right) + 2 c_2 x_0 z_0^2 f_2'(x_0)^2 f_3'(y_0) \\
&+ y_0 \left(d_1 + z_0 f_3'(y_0)\right)^2 \left(z_0 f_3''(y_0) - x_0 f_1''(x_0)\right) , \\
\sigma_{22} =& f_3'(y_0) (2 z_0 f_2'(x_0) \left((z_0 - c_2 x_0) f_3'(y_0) + d_1\right) - x_0 \left(d_1 + z_0 f_3'(y_0)\right) \\
&\times \left(y_0 f_1''(x_0) + z_0 f_2''(x_0)\right)) + y_0 f_3''(y_0) \left(d_1 + z_0 f_3'(y_0)\right)^2 , \\
\sigma_3 =& c_2 z_0 f_2(x_0)^2 f_2'(x_0) \left(d_1 + z_0 f_3'(y_0)\right) + c_2 x_0^2 y_0 z_0 f_1'(x_0) f_2'(x_0) f_3'(y_0)^2 \\
&+ y_0 f_2(x_0) f_1'(x_0) \left(d_1 + z_0 f_3'(y_0)\right)^2 , \\
\theta_1 =& - c_2 x_0 z_0 f_2'(x_0) \left(f_2'(x_0) \left(d_1 - z_0 f_3'(y_0)\right) + x_0 f_3'(y_0) \left(y_0 f_1''(x_0) + z_0 f_2''(x_0)\right)\right) \\
&+ y_0 z_0 f_3''(y_0) \left(d_1 + z_0 f_3'(y_0)\right) \left(-c_2 x_0 f_2'(x_0) + d_1 + z_0 f_3'(y_0)\right) + y_0 f_1'(x_0) \\
&\times \left(d_1^2 - z_0^2 f_3'(y_0)^2\right) , \\
\theta_2 =& f_1'(x_0) \left(f_2'(x_0) \left(z_0 (c_2 x_0 - z_0) f_3'(y_0)^2 + d_1^2\right) + x_0 f_3'(y_0) \theta_{21}\right) \\
&- c_2 x_0 z_0 f_2'(x_0) f_3'(y_0)^2 \left(x_0 f_1''(x_0) + z_0 f_3''(y_0)\right) , \\
\theta_{21} =& z_0 f_2''(x_0) \left((c_2 x_0 + z_0) f_3'(y_0) + d_1\right) + y_0 f_1''(x_0) \left(d_1 + z_0 f_3'(y_0)\right) , \\
\theta_3 =& c_2 z_0 f_2(x_0)^3 f_2'(x_0) \left(d_1 - z_0 f_3'(y_0)\right) + c_2 x_0^3 y_0 z_0 f_1'(x_0) f_2'(x_0)^2 f_3'(y_0)^2 , \\
\theta_4 =& x_0 f_1'(x_0) f_2''(x_0) \left(d_1 f_2(x_0) + z_0 \left(f_2(x_0) - x_0 f_2'(x_0)\right) f_3'(y_0)\right) \\
&+ f_2'(x_0) (2 d_1 f_1'(x_0) \left(f_2(x_0) - x_0 f_2'(x_0)\right) \\
&- x_0 f_1''(x_0) \left(d_1 f_2(x_0) + f_3'(y_0) \left(x_0 y_0 f_1'(x_0) + z_0 f_2(x_0)\right)\right)).
\end{aligned}
$$

B. Second nondegeneracy condition

$$
\begin{aligned}
\Delta =& x_0 f_1'(x_0) (\Delta_1) - z_0 f_2'(x_0) f_3''(y_0) \left(x_0 f_2'(x_0) + k_2\right) \left(d_1 + z_0 f_3'(y_0)\right) (\Delta_2) \\
&- x_0^2 y_0 f_1'(x_0)^2 f_3'(y_0)^2 \left(d_1 + z_0 f_3'(y_0)\right) \left(k_2 f_2'(x_0) + x_0 f_2''(x_0) \left(x_0 f_2'(x_0) + k_2\right)\right) , \\
\Delta_1 =& y_0 f_3''(y_0) \left(f_2'(x_0) (\Delta_{11}) + x_0 f_2'(x_0)^2 \left(d_1 + z_0 f_3'(y_0)\right) (\Delta_{12}) + \Delta_{13}\right) \\
&- f_2'(x_0) f_3'(y_0) (x_0 f_2'(x_0) + k_2) (d_1 + z_0 f_3'(y_0)) \left(z_0 f_3'(y_0) \left(x_0^2 f_2''(x_0) + k_2\right) - d_1 k_2\right) , \\
\Delta_2 =& x_0 \big(- f_3'(y_0) (\Delta_{21}) + f_2'(x_0) \left(3 d_1 k_2 - f_3'(y_0) (\Delta_{22})\right)
\end{aligned}
$$

$$
\begin{aligned}
&\quad + x_0 f_2'(x_0)^2 \left(d_1 + z_0 f_3'(y_0)\right)\Big) + 2gd_1k_2^2, \\
\Delta_{11} =& - 2d_1^2k_2^2 + d_1k_2f_3'(y_0)\left(x_0^2\left(y_0f_1''(x_0) + z_0f_2''(x_0)\right) - 2k_2z_0\right) \\
&+ x_0z_0f_3'(y_0)^2\left(x_0f_2''(x_0)(d_1x_0 + k_2z_0) + 3d_1k_2 + k_2x_0y_0f_1''(x_0)\right) \\
&+ x_0z_0f_3'(y_0)^3\left(k_2z_0 - x_0^2y_0f_1''(x_0)\right), \\
\Delta_{12} =& f_3'(y_0)\left(x_0\left(x_0y_0f_1''(x_0) + x_0z_0f_2''(x_0) + z_0f_3'(y_0)\right) - k_2z_0\right) - 3d_1k_2, \\
\Delta_{13} =& k_2x_0^2z_0f_2''(x_0)f_3'(y_0)^2\left(d_1 + z_0f_3'(y_0)\right) - x_0^2f_2'(x_0)^3\left(d_1 + z_0f_3'(y_0)\right)^2, \\
\Delta_{21} =& k_2\left(d_1 + x_0y_0f_1''(x_0) + x_0z_0f_2''(x_0)\right) + f_3'(y_0)\left(k_2z_0 - x_0^2y_0f_1''(x_0)\right), \\
\Delta_{22} =& d_1x_0 + x_0\left(x_0y_0f_1''(x_0) + x_0z_0f_2''(x_0) + z_0f_3'(y_0)\right) - k_2z_0.
\end{aligned}
$$

References

[1] F. Capone, M. Carfora and R. D. Luca, *On the dynamics of an intraguild predator-prey model*, Math. Comput. Simulation, 2018, 149, 17–31.

[2] V. Castellanos, J. Llibre and I. Quilantán, *Simultaneous periodic orbits bifurcating from two zero-Hopf equilibria in a tritrophic food chain model*, J Appl Math Phys., 2013, 1, 31–38.

[3] F. Castillo-Santos, M. Dela-Rosa and I. Loreto-Hernández, *Existence of a Limit Cycle in an Intraguild Food Web Model with Holling Type II and LogisticGrowth for the Common Prey*, Applied Mathematics, 2017, 8, 358–376.

[4] J. H. P. Dawes and M. O. Souza, *A derivation of Holling's type I, II and III functional responses in predator–prey systems*, J. of Theor. Biol., 2013, 327, 11–22.

[5] J. Ginoux and J. Llibre, *Zero-Hopf bifurcation in the Volterra-Gause system of predator-prey type*, Math. Methods Appl. Sci., 2017, 40(18), 7858–7866.

[6] J. Guckenheimer and P. Holmes, *Nonlinear Oscillations, Dynamical Systems, and Bifurcations of Vector Fields*, Springer-Verlag, New York, 1983.

[7] J. Guckenheimer and Y. A. Kuznetsov, *Fold–Hopf bifurcation*, Scholarpedia, 2007, 2(10), 1855.

[8] C. S. Holling, *Some characteristics of simple types of predation and parasitism*, Can. Entomol., 1959, 91, 385–398.

[9] R. D. Holt and G. A. Polis, *A theoretical framework for intraguild predation*, Am. Nat., 1997, 149(4), 745–764.

[10] Y. Kang and L. Wedekin, *Dynamics of a intraguild predation model with generalist or specialist predator*, J. Math. Biol., 2013, 67, 1227–1259.

[11] M. H. Khan and Z. Yoldaş, *Intraguild predation between two aphidophagous coccinellids, Hippodamia variegata (G.) and Coccinella septempunctata L.(Coleoptera: Coccinellidae): the role of prey abundance*, Biological Control, 2018, 126, 7–14.

[12] Y. A. Kuznetsov, *Elements of applied Bifurcation Theory*, 3rd Edn, Springer-Verlag, 2004.

[13] H. Liu, T. Li and F. Zhangi, *A prey-predator model with Holling II functional response and the carrying capacity of predator depending on its prey*, J. Appl. Anal. Comput., 2018, 8(5), 1464–1474.

[14] J. P. Mendonça, I. Gleria and M. L. Lyra, *Prey refuge and morphological defense mechanisms as nonlinear triggers in an intraguild predation food web*, Communications in Nonlinear Science and Numerical Simulation, 2020, 90, 105373.

[15] T. Okuyama, *Intraguild predation in biological control: consideration of multiple resource species*, BioControl, 2009, 54, 3–7.

[16] L. Petráková, R. Michalko, P. Loverre et al., *Intraguild predation among spiders and their effect on the pear psylla during winter*, Agriculture, Ecosystems & Environment, 2016, 233, 67–74.

[17] G. A. Polis, C. A. Myers and R. D. Holt, *The ecology and evolution of intraguild predation: Potential competitors that eat each other*, Annual Review of Ecology and Systematics, 1989, 20(1), 297–330.

[18] H. M. Safuan, H. S. Sidhu, Z. Jovanoski and I. N. Tower, *A two-species predator-prey model in an environment enriched by a biotic resource*, ANZIAM J., 2014, 54, 768–787.

[19] D. Sen, S. Ghorai and M. Banerjee, *Complex dynamics of a three species prey-predator model with intraguild predation*, Ecological Complexity, 2018, 34, 9–22.

[20] J. Wang and W. Jiang, *Hopf-zero bifurcation of a delayed predator-prey model with dormancy of predators*, J. Appl. Anal. Comput., 2017, 7(3), 1051–1069.

[21] P. Yang, *Hopf bifurcation of an age-structured prey-predator model with Holling type II functional response incorporating a prey refuge*, Nonlinear Anal. Real World Appl., 2019, 49, 368–385.

[22] P. Yang and Y. Wang, *Hopf-zero bifurcation in an age-dependent predator-prey system with Monod-Haldane functional response comprising strong Allee effect*, J. Differential Equations, 2020, 269(11), 9583–9618.